

Atomic and nuclear physics

Electron shell



Normal Zeeman effect

SPECTROSCOPY WITH A FABRY-PÉROT ETALON

- Measuring Fabry-Pérot etalon interference rings relative to an external magnetic field
- Determining the Bohr magneton

UE5020700-2

07/18 UD

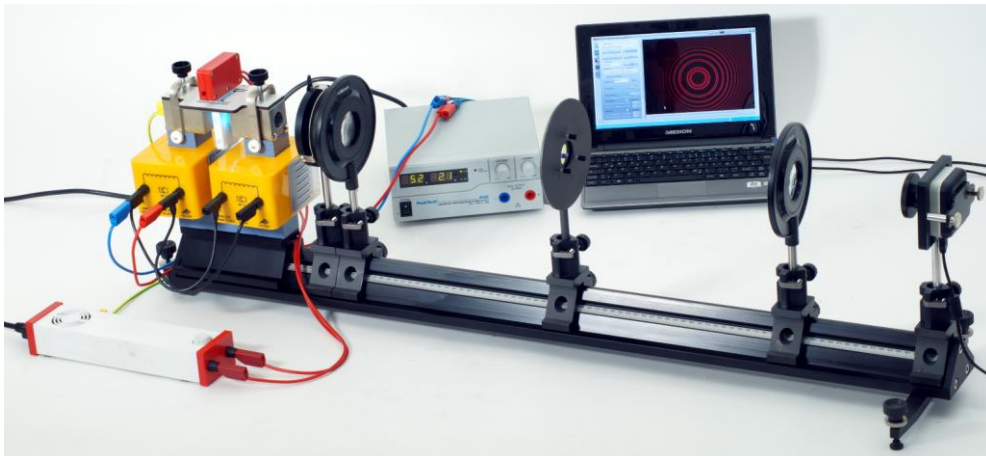


Fig. 1: Measurement arrangement for the longitudinal Zeeman effect

BACKGROUND

The Zeeman effect refers to the splitting of atomic energy levels or spectral lines due to the action of an external magnetic field. Named after P. Zeeman, the scientist who discovered it in 1896, it was classically explained by H. A. Lorentz by means of the Lorentz force that the magnetic field exerts on an electron orbiting the nucleus. In this so-called "normal" Zeeman effect, the spectral line splits into a line doublet (longitudinal Zeeman effect) parallel to the magnetic field and a line triplet (transversal Zeeman effect) perpendicular to the magnetic field. The term "anomalous" Zeeman effect refers to more complex splitting phenomena that remained unexplained till Goudsmit and Uhlenbeck postulated the existence of electron spin

in 1925. Quantum mechanically, the anomalous Zeeman effect relates to the interaction of the magnetic field with the electron shell's magnetic moment generated by the orbital angular momentum and spin of the electrons. In this regard, the anomalous Zeeman effect represents the normal case and the normal Zeeman effect represents a special case.

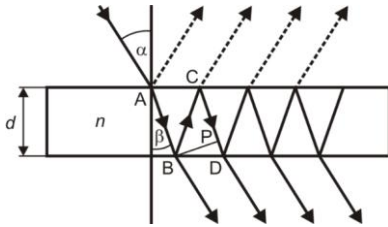


Fig. 2: Beam path in the Fabry-Pérot etalon

For a theoretical description of the normal Zeeman effect, please refer to the instruction manual for the first part of the experiment (UE5020700-1).

This second part of the experiment focuses on spectroscopy with a Fabry-Pérot etalon. The Fabry-Pérot etalon is installed upstream together with imaging optics of the digital camera used to observe the Zeeman splitting phenomenon. As it passes through the Fabry-Pérot etalon, the light from the cadmium lamp creates interference rings that split like the spectral lines according to the external magnetic field and are recorded by the optics of the digital camera. The electromagnets can be rotated on their axes to permit observation parallel or perpendicular to the external magnetic field.

A Fabry-Pérot etalon is an optical resonator comprising a quartz plate with highly reflective, half-silvered mirror finish on both sides (Fig. 2). In the present case, the etalon is designed to meet the resonance conditions for the wavelength $\lambda = 643.8 \text{ nm}$ of the red CD line. In that respect, the etalon also acts as an optical filter. The thickness d , the refractive index n and the reflection coefficient R of the etalon are:

$$d = 4 \text{ mm}$$

$$(1) \quad n = 1,4567$$

$$R = 0,85$$

In the etalon, an incident beam of light is reflected multiple times. The light beams transmitted with each reflection interfere with one another. The path difference Δs between adjacent transmitted light beams, e.g. the light beams emitted at points B and D in Fig. 2 is:

$$(2) \quad \Delta s = n \cdot (\overline{BC} + \overline{CP}).$$

Given

$$(3) \quad \overline{CP} = \overline{BC} \cdot \cos(2 \cdot \beta),$$

$$(4) \quad d = \overline{BC} \cdot \cos(\beta),$$

Snell's law of refraction ($n_{\text{air}} \approx 1$)

$$(5) \quad \sin(\alpha) = n \cdot \sin(\beta)$$

and the addition theorems

$$(6) \quad \cos(\beta) = \sqrt{1 - \sin^2(\beta)}$$

$$\cos(2 \cdot \beta) = 1 - 2 \cdot \sin^2(\beta)$$

the path difference is

$$(7) \quad \Delta s = 2 \cdot d \cdot \sqrt{n^2 - \sin^2(\alpha)} = 2 \cdot d \cdot n \cdot \cos(\beta)$$

and from that the condition for the existence of interference maxima is:

$$(8) \quad k \cdot \lambda = 2 \cdot d \cdot \sqrt{n^2 - \sin^2(\alpha_k)} = 2 \cdot d \cdot n \cdot \cos(\beta_k).$$

k : Whole number, order of interference

α_k : Angle of incidence to the k^{th} order of interference

β_k : Angle of refraction to the k^{th} order of interference

Together, this generates an interference pattern comprising concentric rings. Refraction at the boundary surfaces of the Fabry-Pérot etalon glass plate is negligible because it only shifts the interference pattern in parallel. For this reason, the angle of refraction β is replaced by the angle of incidence α , and the interference condition (8) results in

$$(9) \quad k \cdot \lambda = 2 \cdot d \cdot n \cdot \cos(\alpha_k) \approx 2 \cdot d \cdot n \cdot \left(1 - \frac{\alpha_k^2}{2}\right),$$

with the development $\cos(x) \approx (1 - x^2 / 2)$ of the cosine function.

The convex lens is used to reproduce the interference pattern on the digital camera (Fig. 3). The following relationship exists between the angle α_k under which the interference ring to the k^{th} order appears, the radius r_k of the interference ring to the k^{th} order and the focal length f of the lens (Fig. 3):

$$(10) \quad r_k = f \cdot \tan(\alpha_k) \approx f \cdot \alpha_k,$$

with the small-angle approximation $\tan(x) \approx x$. For the order of interference k and the angle α_k , equation (9) gives

$$(11) \quad k = k_0 \cdot \cos(\alpha_k) \approx k_0 \cdot \left(1 - \frac{\alpha_k^2}{2}\right) \text{ with } k_0 = \frac{2 \cdot d \cdot n}{\lambda}$$

and

$$(12) \quad \alpha_k = \sqrt{\frac{2 \cdot (k_0 - k)}{k_0}}.$$

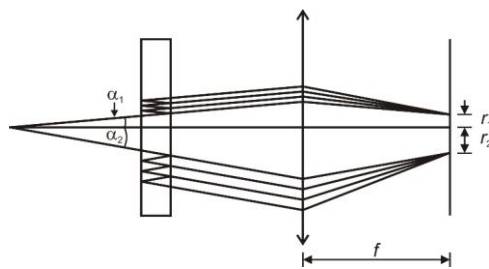


Fig. 3: Reproduction of Fabry-Pérot etalon interference rings on the digital camera

According to equation (11), since $|\cos(\alpha_k)| \leq 1$, the order of interference k is the greatest for $\alpha_k = 0$, i.e. at the centre of the interference rings. In that case, it also corresponds to the parameter k_0 , which is generally not a whole number. Since the interference rings in the experiment are numbered from the centre outward, the order of interference k is indexed with a whole number j , which identifies the k^{th} order of interference with the j^{th} interference ring counting from the centre outward, by generalisation of the parameter k_0 already introduced.

According to equation (12), the first bright interference ring with the order k appears under the angle

$$(13) \alpha_{k_1} = \sqrt{\frac{2 \cdot (k_0 - k_1)}{k_0}},$$

whereby k_1 is the next whole number smaller than k_0 . Since k_0 is not a whole number in general, the difference $k_0 - k_1$ is less than 1. For this reason, a parameter ε is defined as follows:

$$(14) \varepsilon := k_0 - k_1 \text{ with } 0 < \varepsilon < 1$$

For all interference rings with $j \geq 2$, the order number k_i decreases by 1, so for the order of interference of the j^{th} interference ring counting outward from the centre, the following generally applies:

$$(15) k_j = (k_0 - \varepsilon) - (j - 1)$$

For $j = 1$, equation (15) corresponds directly to the definition of ε from equation (14). Substituting equation (12) with $k = k_j$ and equation (15) into equation (10) gives

$$(16) r_j = \sqrt{\frac{2 \cdot f^2}{k_0} \cdot \sqrt{(j-1) + \varepsilon}},$$

whereby for simplicity of indexing, without restricting general applicability, the convention $r_{k_i} \rightarrow r_j$ was set. This convention will be maintained hereafter. From equation (16), it follows that the difference between the squared radii of adjacent interference rings is constant:

$$(17) r_{j+1}^2 - r_j^2 = \frac{2 \cdot f^2}{k_0} = \text{const.}$$

From equation (16) and (17), it follows that:

$$(18) \varepsilon = \frac{r_{j+1}^2}{r_{j+1}^2 - r_j^2} - j.$$

If the interference rings split into two very closely adjacent components a and b , whose wavelengths differ from one another only slightly, then according to equation (14) it follows, for example, for the first interference ring counting outward from the centre:

$$(19) \begin{aligned} \varepsilon_a &= k_{0,a} - k_{1,a} = \frac{2 \cdot d \cdot n}{\lambda_a} - k_{1,a} \\ \varepsilon_b &= k_{0,b} - k_{1,b} = \frac{2 \cdot d \cdot n}{\lambda_b} - k_{1,b} \end{aligned}$$

Since the two components belong to the same order of interference, provided that the interference rings do not overlap by more than one whole order, then $k_{1,a} = k_{1,b}$ and thus:

$$(20) \varepsilon_a - \varepsilon_b = k_{0,a} - k_{0,b} = 2 \cdot d \cdot n \cdot \left(\frac{1}{\lambda_a} - \frac{1}{\lambda_b} \right).$$

Equation (20) does not explicitly depend on the order of interference. Formulating equation (18) for the two components a and b and substituting it into equation (20) gives:

$$(21) \left(\frac{1}{\lambda_a} - \frac{1}{\lambda_b} \right) = \frac{1}{2 \cdot d \cdot n} \cdot \left(\frac{r_{j+1,a}^2}{r_{j+1,a}^2 - r_{j,a}^2} - \frac{r_{j+1,b}^2}{r_{j+1,b}^2 - r_{j,b}^2} \right).$$

Since $\lambda_a \approx \lambda_b$ and therefore $k_{0,a} \approx k_{0,b}$, it follows from equation (17) that, with $j > 0$, the differences between the radii squared of component a or b for adjacent orders of interference j and $j+1$ are approximately equal:

$$(22) \Delta_a^{j+1,j} = r_{j+1,a}^2 - r_{j,a}^2 = r_{j+1,b}^2 - r_{j,b}^2 = \Delta_b^{j+1,j}.$$

Accordingly, for two components a and b of the same order of interference j with $j > 0$:

$$(23) \delta_{a,b}^j = r_{j,a}^2 - r_{j,b}^2 = r_{j+1,a}^2 - r_{j+1,b}^2 = \delta_{a,b}^{j+1}.$$

Substituting equations (22) and (23) into equation (21) gives:

$$(24) \left(\frac{1}{\lambda_a} - \frac{1}{\lambda_b} \right) = \frac{1}{2 \cdot d \cdot n} \cdot \frac{\delta_{a,b}^{j+1}}{\Delta_a^{j+1,j}} \text{ for all } j > 0$$

Since equation (22) applies for the two components a and b of adjacent interference rings and equation (23) applies for all interference rings, the mean values

$$(25) \delta = \overline{\delta_{a,b}^j}$$

and

$$(26) \Delta = \overline{\Delta_a^{j+1,j}}$$

can be formed and substituted into equation (24):

$$(27) \left(\frac{1}{\lambda_a} - \frac{1}{\lambda_b} \right) = \frac{1}{2 \cdot d \cdot n} \cdot \frac{\delta}{\Delta}.$$

with

$$(28) \Delta E_{a,b} = h \cdot c \cdot \left(\frac{1}{\lambda_a} - \frac{1}{\lambda_b} \right) = \mu_B \cdot B$$

it follows from equation (27) that:

$$(29) \frac{\delta}{\Delta} = \frac{2 \cdot d \cdot n \cdot \mu_B}{h \cdot c} \cdot B = m \cdot B \text{ with } m := \frac{2 \cdot d \cdot n}{h \cdot c} \cdot \mu_B.$$

The quotient δ / Δ can be measured and graphically represented as a function of magnetic flux density B , and the Bohr magneton μ_B can be determined from the slope m of a trend line.

EQUIPMENT LIST

1	Cd lamp with accessories @230V	1021366 (U8557780-230)
or		
1	Cd lamp with accessories @115V	1021747 (U8557780-115)
1	U-shaped core D	1000979 (U8497215)
2	Coils D 900 taps	1012859 (U8497390)
1	Electromagnet accessories for Zeeman effect	1021365 ()
1	DC power supply 1 – 32 V, 0 – 20 A @230V	1012857 (U11827-230)
In countries with 110 – 120 V mains, a power supply that corresponds to power supply 1012857 is required.		
1	Set of 15 experiment leads, 75 cm, 1mm ²	1002840 (U13800)
1	Fabry-Pérot etalon	1020903 (U8557590)
2	Convex lenses on rod, f = 100 mm	1003023 (U17102)
1	Quarter-wavelength plate on rod	1021353 (U22023)
1	Polarising attachment	1021364 (U8557760)
1	Polarisation filter on rod	1008668 (U22017)
1	Optical bench D, 100 cm	1002628 (U10300)
1	Set of feet for optical bench D	1012399 (U103041)
1	Optical base D	1009733 (U10319)
5	Optical slider D 90/36	1012401 (U103161)
1	Holder and filter for Moticam	1021367 (U8557790)
1	Digital camera Moticam 1	1021162 (U13160)

SET-UP AND SAFETY INSTRUCTIONS

Before this second part of the experiment can be carried out, the components must be installed and the experiment must be set-up and adjusted as described in the instruction manual for the first part of the experiment, observing all safety instructions therein.

PROCEDURE

Calibration of the electromagnet

For the evaluation described here, the relationship of the magnetic field strength to the current through the coils must be known. For this reason, the following calibration must be performed.

- Remove the Cd lamp on the housing from the mounting plate.
- Place a gaussmeter (not included with the equipment supplied) in the air gap between the two pole pieces (approx. 10 mm), with the magnetic field sensor centred in the gap.
- Switch on the DC power supply and raise the current I supplied to the coils in increments (e.g. 1 A). Set the maximum current to 5 A for no more than 7 minutes and higher currents up to 10 A for no more than 10 seconds. Measure and record the value of the magnetic flux density B for each increment, and graph the results versus the

respective values of current.

An example of a calibration curve is shown in Fig. 5.

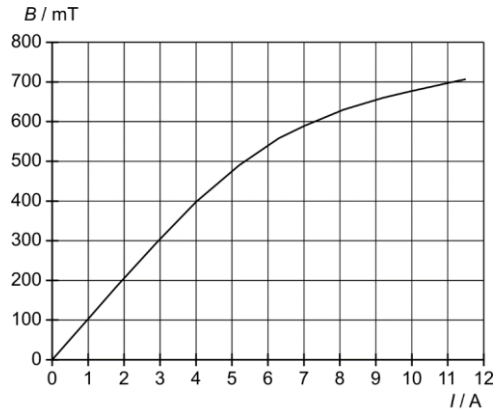



Fig. 5: Calibration curve of the electromagnet

Measurement

- Set up the transversal configuration by turning the electromagnet as described in part 1 of the experiment instruction manual.
- Reduce the current to zero and switch off the DC power supply.
- Re-install the Cd lamp in the mounting plate.
- Switch on the DC power supply, raise the current supplied to the coils to 3 A, and capture a single image with the camera software.
- To do so, click on the  button in the Live Image Module and then click on "Capture". Switch from the Live Image Module to the main display. The recorded capture appears large in the display and also small in the preview window. Click on "File" → "Save as" in the menu bar to save the file under a descriptive name.
- Increase the current, e.g. in 0.5-A increments, up to 5 A, and capture and save a single image with the camera software for each increment.

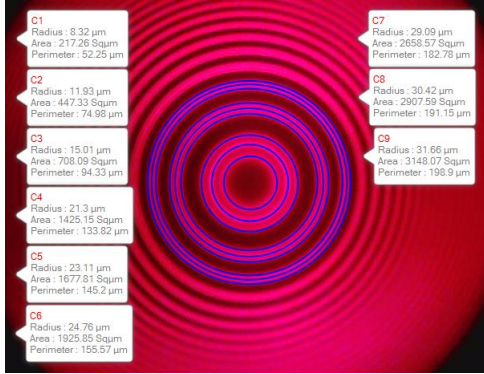


Fig. 4: Triplet splitting of the red cadmium line ($I = 3.5 \text{ A} \triangleq B = 340 \text{ mT}$) and use of the camera software to determine the areas enclosed by the interference rings

Note
When increasing the current, make sure that the interference rings do not overlap by more than one whole order.

MEASUREMENT EXAMPLE AND EVALUATION

- In the main display of the camera software, select a capture from the preview window, so it appears in large for-

Tab. 1: Areas enclosed by the interference rings as determined by means of the camera software ($I = 3.5 \text{ A} \triangleq B = 340 \text{ mT}$)

j	Component	Circle	Area / μm^2
1	σ^-	C1	217
	π	C2	447
	σ^+	C3	708
2	σ^-	C4	1425
	π	C5	1678
	σ^-	C6	1926
3	σ^-	C7	2659
	π	C8	2908
	σ^+	C9	3148

Tab. 2: Differential areas Δ of corresponding components of adjacent orders of interference ($I = 3.5 \text{ A} \triangleq B = 340 \text{ mT}$)

Differential area Δ / μm^2	
$\Delta_{C4,C1}$	1208

mat on the display.

- In the menu list on the right, click on "Measure" and select "Circle". Click in the centre of the interference rings one after another, draw circles, and align them with as many interference rings as possible.

Fig. 4 illustrates the evaluation of recorded capture for $I = 3.5 \text{ A} \triangleq B = 340 \text{ mT}$. For each circle drawn, a text field appears listing the values of the radius, area and perimeter of that circle.

- Record the areas of all circles in Tab. 1.

The unit of area is irrelevant to the subsequent analysis, because only relative values will be computed, not absolute ones.

- Calculate the differential areas Δ of components of adjacent orders of interference (circles C4/C1, C5/C2, C6/C3, C7/C4, C8/C5, C9/C6) and enter them into Tab. 2.
- Calculate the differential areas δ of adjacent components of the same orders of interference (circles C2/C1, C3/C2, C5/C4, C6/C5, C8/C7, C9/C8) and enter them into Tab. 3.
- Determine the respective means of all differential areas in Tab. 2 and 3 and enter them into the tables.

$\Delta_{C5,C2}$	1231
$\Delta_{C6,C3}$	1218
$\Delta_{C7,C4}$	1234
$\Delta_{C8,C5}$	1230
$\Delta_{C9,C6}$	1222
Mean	1224

Tab. 3: Differential areas δ of adjacent components of the same orders of interference ($I = 3.5 \text{ A} \triangleq B = 340 \text{ mT}$)

Differential area δ / μm^2	
$\delta_{C2,C1}$	230
$\delta_{C3,C2}$	261
$\delta_{C5,C4}$	253
$\delta_{C6,C5}$	248
$\delta_{C8,C7}$	249
$\delta_{C9,C8}$	240
Mean	247

Tab. 4: Ratio δ / Δ of differential areas for different currents I and magnetic flux densities B

I / A	B / mT	δ / Δ
3,0	301	0,168
3,5	340	0,202
4,0	392	0,211
4,5	431	0,241
5,0	473	0,271

- Carry out the evaluation described above for all captures recorded at the other currents and magnetic flux densities.
- Calculate the quotients δ / Δ of the means for all currents and magnetic flux densities and enter them into Tab. 4 (e.g. $\delta / \Delta = 0.202$ for $I = 3.5 A \hat{=} B = 340 mT$). Take the corresponding values of magnetic flux density from the calibration curve of the electromagnet established in the first part of the experiment.
- Graph the quotients δ / Δ as a function of magnetic flux density B and draw a best-fit line through the origin (Fig. 5).
- Use equation (29) to determine the Bohr magneton from the slope $m = 0.56 / T$ of the best-fit line:

$$\begin{aligned} \mu_B &= \frac{h \cdot c \cdot m}{2 \cdot d \cdot n} \\ (30) &= \frac{6,6 \cdot 10^{-34} \text{ Js} \cdot 3,0 \cdot 10^8 \text{ m/s} \cdot 0,56 / T}{2 \cdot 4 \text{ mm} \cdot 1,4567} \\ &= 9,6 \cdot 10^{-24} \frac{\text{J}}{\text{T}} \end{aligned}$$

The value falls within 3% of the theoretical value $9.3 \cdot 10^{-24} \text{ J/T}$.

Kommentiert [otc1]: In Gleichung 30 und in Fig. 5., Dezimalkommas durch Punkte ersetzen.

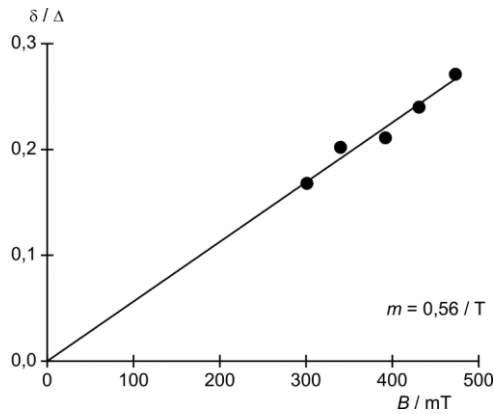


Fig. 5: Quotient δ / Δ as a function of magnetic flux density B